Journal of Infrastructure Planning and Engineering

Journal homepage: ejournal.warmadewa.ac.id

e-ISSN: 2829-5153

Evaluation of drainage capacity for various design discharges in the downstream Cibeber river

Andhika Bayu Kristanto[1], Teguh Eko Saputro*[1]

[1]*Department of Civil Engineering, Universitas Serang Raya, Serang, 42162, Indonesia*
*teguhekosaputro@unsera.ac.id

Received 22 July 2026; revised 3 October 2026; accepted 12 October 2026; published 20 October 2026

ABSTRACT

Urban flooding in the Sukmajaya area of Cilegon frequently occurs during heavy rainfall, yet the hydraulic interaction between the local drainage network and the Cibeber River has not been comprehensively evaluated. This study aims to assess the hydraulic performance of the existing drainage system under various design flood scenarios and to identify the dominant mechanism governing flood occurrence. Hydrological inputs were derived using the Nakayasu Synthetic Unit Hydrograph and the Mononobe rainfall distribution method, while one-dimensional unsteady-flow simulations were performed in HEC-RAS based on field-surveyed channel geometries and high-resolution geospatial datasets. The results indicate that flooding is primarily influenced by downstream backwater effects, while local channel capacity limitations also contribute at specific locations. Under the 50-year design flood, corresponding to a peak inflow of 84.92 m^3/s, the water level at the Kubang Laban–Cibeber junction reached a maximum of 5.46 m and remained above the existing channel-bank elevation for approximately 16 hours. During the critical period, reverse flow at the Kubang Laban junction reached -2.02 m^3/s, indicating a reversal of flow direction from the Cibeber River toward the local drainage network. These conditions restricted gravity-driven drainage and promoted prolonged inundation within the urban drainage network. Based on these findings, this study recommends an integrated polder system comprising continuous levees, temporary retention storage, and mechanical pumping to interrupt hydraulic connectivity with the receiving river and improve drainage performance during extreme flood events. The proposed framework provides a practical reference for flood mitigation in urban areas affected by river-induced backwater.

Keywords: backwater effect; urban drainage; HEC-RAS; flood mitigation; polder system

1 Introduction

Rapid urban development and land use changes have transformed natural watersheds into built-up areas dominated by impervious surfaces [1]. This Land Use and Land Cover (LULC) transformation shows a linear relationship with increased surface runoff generation [2]. Such land use changes drastically increase peak surface runoff discharge [3], while urbanization significantly influences the magnitude of peak flows [4]. Furthermore, climate change is expected to increase the frequency and intensity of extreme rainfall events, posing additional challenges to urban drainage system design [5]. Consequently, urban drainage systems are subjected to increasing hydraulic loads, often resulting in localized flooding even when the primary drainage channels appear hydraulically adequate [6].

Urban inundation is often exacerbated by hydraulic interactions between local drainage networks and receiving rivers, which may compromise the hydraulic performance of urban drainage systems [7]. When river water levels exceed the elevation of drainage outlets, submerged outflow conditions may occur, substantially reducing drainage capacity and even triggering reverse flow into the drainage system [6]. Such downstream hydraulic conditions generate backwater effects that impair the conveyance performance of urban drainage networks, even when the channel dimensions are theoretically adequate [8]. Experimental studies have demonstrated that backwater conditions reduce flow velocity, decrease energy dissipation, and promote upstream ponding, thereby prolonging flood recession [9]. These findings highlight the importance of incorporating downstream hydraulic conditions into

https://doi.org/10.22225/jipe.5.2.2026.93-104

2829-5153 ©2026 The Author(s). Published by Master Program of Infrastructure and Environmental Engineering, Postgraduate Program, Warmadewa University. This is an open access article CC BY-SA license (https://creativecommons.org/licenses/by-sa/4.0/)

How to Cite: A. B. Kristanto and T. E. Saputro, "Evaluation of drainage capacity for various design discharges in the downstream Cibeber river," *Journal of Infrastructure Planning and Engineering*, vol. 5, no. 2, pp. 93 - 104, October, 2026.

urban drainage performance assessments to support effective flood mitigation planning [10].

Numerical modeling has become an essential tool for evaluating the performance of urban drainage systems under various hydrological conditions [11]. Among the available modeling tools, HEC-RAS has been widely applied to simulate flow behavior, assess channel conveyance capacity, and support flood mitigation planning in urban environments [8], [11]. However, previous studies have predominantly emphasized evaluating drainage channel capacity or investigating backwater impacts independently [8], [11]. Comparatively fewer studies have quantitatively differentiated whether urban inundation is predominantly controlled by insufficient local drainage capacity or by downstream influences associated with submerged outflow and backwater conditions. This limitation highlights the need for integrated assessments that simultaneously evaluate local drainage performance and downstream river conditions to accurately identify the dominant flow mechanisms responsible for urban inundation.

The Sukmajaya area, particularly the Kranggot area in Cilegon, Indonesia, frequently experiences inundation during periods of high-intensity rainfall [12], [13], [14]. Field observations indicate that discharge from the local drainage outlets into the Cibeber River becomes restricted during these events. However, the relative contribution of local drainage capacity and downstream hydraulic conditions to the observed inundation has not yet been quantitatively evaluated. Therefore, this study aims to investigate the interaction between the local drainage network and the Cibeber River under various design flood scenarios using one-dimensional hydraulic modeling. The findings are expected to provide a quantitative basis for evaluating the performance of the existing drainage system and supporting the development of flood mitigation strategies.

2 Data and Methods

2.1 Study Location and Time

This study was conducted in the Sukmajaya area, focusing on the Kranggot neighborhood and the downstream reach of the Cibeber River in Cilegon City, Banten Province, Indonesia, as shown in **Figure 1**. The study area covers approximately 0.86 km^2, while the hydrological analysis was performed using the 34.26 km^2 Cibeber Subwatershed as the contributing catchment for design flood estimation. The area is characterized by relatively flat topography, with ground elevations generally below 16 m above mean sea level, and is drained through a hierarchical urban drainage system in which tertiary channels discharge into secondary channels before ultimately conveying flow to the downstream reach of the Cibeber River via the Kubang Laban Secondary Channel. The study area was selected because recurrent inundation has been reported during high-intensity rainfall events, suggesting potential hydraulic interaction between the local drainage network and the downstream river. Field surveys, hydrological and hydraulic data collection, and numerical simulations were conducted between March and July 2026.

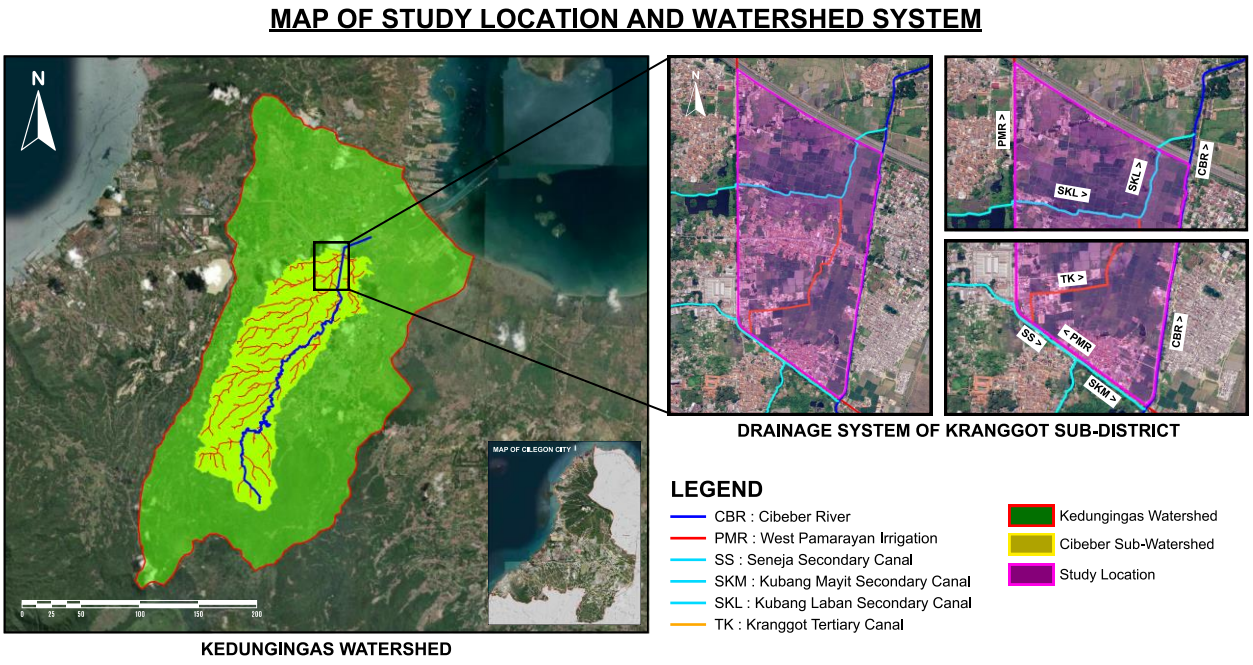


Figure 1. Map of the study location

2.2 Data Collection

The hydraulic assessment of the urban drainage system required the integration of primary and secondary datasets to ensure that the hydrodynamic simulations realistically represented the existing flow conditions.

Primary data were collected through field surveys to obtain the actual cross-sectional dimensions, longitudinal profiles, and physical conditions of the existing drainage channels. Field observations were also conducted to estimate channel roughness coefficients (Manning's n) and identify critical hydraulic junctions and drainage inlets governing flow distribution within the network. The Manning's n values used in the model ranged from 0.02–0.04 for the main channel areas and 0.014–0.03 for the overbank areas. These values were assigned based on observed surface conditions and reference values reported by Chow (1959) [15] .

Secondary data comprised engineering records from the Department of Public Works and Spatial Planning (DPUPR) of Cilegon City and publicly available geospatial datasets. The engineering records included channel inventories, drainage alignments, and KML-based spatial data used to define the drainage geometry and network connectivity. Long-term daily rainfall records were obtained from the Serang Class I Maritime Meteorology Station (BMKG) and the Cidanau–Ciujung–Cidurian River Basin Organization (BBWS C3) for hydrological analysis and design flood estimation.

High-resolution geospatial datasets, including DEMNAS and ESA WorldCover V2 2021, were processed using ArcGIS Pro. DEMNAS was used to delineate the Cibeber Subwatershed boundary [16], whereas ESA WorldCover V2 2021 was employed to characterize land use within the delineated catchment [17]. The resulting land-use map is presented in **Figure 2**, while a summary of the datasets, their sources, and applications is provided in **Table 1**.

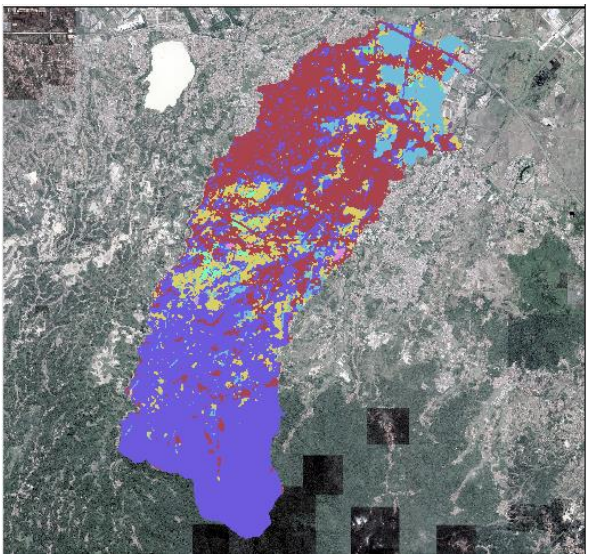


Figure 2. Land Use and Land Cover (LULC) delineation map of the cibeber sub-watershed derived from ESA WorldCover V2 2021

Table 1. Summary of primary and secondary data for hydrological and hydraulic analysis

Data Type	Description and Resolution	Source	Purpose
Channel Geometry	Measured cross-sectional dimensions of the Kranggot tertiary channel, Kubang Laban, Kubang Mayit, Seneja secondary channels, and the Cibeber River	Direct field measurement	Hydraulic geometry input for HEC-RAS model development
Topographic Data	Digital Elevation Model Nasional (DEMNAS) with 8-meter spatial resolution	Geospatial Information Agency (BIG)	Cibeber subwatershed delineation
Land Use Data	ESA WorldCover V2 2021 with 10-meter spatial resolution	European Space Agency (ESA)	Land-use characterization and runoff coefficient determination
Rainfall Data	Historical daily rainfall data (2016–2025) from Serang, Puloampel, Sukmajaya, and Cinangka rainfall stations	BMKG Maritime Station Class 1 Serang and BBWS Cidanau-Ciujung-Cidurian (BBWS C3)	Frequency analysis and design flood estimation
Drainage Masterplan	Drainage network inventory, channel alignment, and flow connectivity	DPUPR of Cilegon City	Drainage network verification and hydraulic model configuration

2.3 Hydrological and Hydraulic Framework

Prior to hydrological analysis, the rainfall records were preprocessed to ensure data completeness and consistency. Missing rainfall values were estimated using the Normal Ratio method, while data consistency was verified through the Double Mass Curve (DMC) analysis. Subsequently, areal rainfall over the Cibeber Subwatershed was determined using the Thiessen Polygon method, which is appropriate for watersheds with irregularly distributed rainfall stations.

The determination of the design rainfall necessitates a frequency analysis. The selection of the appropriate probability distribution—such as Normal, Log-Normal, Gumbel, or Log Pearson Type III—was strictly dictated by the statistical parameters of the data, specifically the coefficients of skewness (Cs) and kurtosis (Ck). Based on the statistical characteristics of the rainfall dataset, the Log Pearson Type III distribution satisfied the selection criteria and was therefore adopted for estimating design rainfall [18]. The distribution is mathematically expressed as:

$$\log X_T = \overline{\log X} + K \cdot S_{\log X} \quad (1)$$

where $\log X_T$ is the logarithm of the design rainfall for a specific return period (T), $\overline{\log X}$ is the mean of the logarithmic rainfall values, K is the frequency factor dependent on the skewness coefficient, and $S_{\log X}$ is the standard deviation. The selected distribution was subsequently verified using the Chi-Square and Smirnov-Kolmogorov goodness-of-fit tests in accordance with SNI 2415:2026 [18].

Since the Nakayasu SUH requires effective rainfall in a temporal distribution, the daily design rainfall was transformed into hourly rainfall intensity using the Mononobe equation [18]. To evaluate the peak discharge, the daily design rainfall must be temporally distributed into hourly intensities. This study adopted the Mononobe intensity formula:

$$I = \frac{R_{24}}{24}\left(\frac{24}{t_c}\right)^{2/3} \quad (2)$$

where I is the rainfall intensity, R_{24} is the maximum daily rainfall, and t_c is the time of concentration.

Considering the heterogeneous land-use composition of the watershed, a composite runoff coefficient was calculated to represent the overall hydrological response of the catchment [18]. Because the watershed consists of varying land-use types, a composite runoff coefficient (C_w) was formulated:

$$C_w = \frac{\sum(C_i \cdot A_i)}{\sum A_i} \quad (3)$$

where C_i and A_i represent the specific runoff coefficient and area for each land-use category, respectively.

The Nakayasu Synthetic Unit Hydrograph was selected because it has been widely applied for design flood estimation in Indonesian watersheds with limited streamflow observations [18], [19]. Based on these calculated parameters, the Nakayasu Synthetic Unit Hydrograph (SUH) was utilized to transform the physical characteristics of the watershed into a design peak discharge. The Nakayasu SUH peak discharge is formulated as:

$$Q_p = \frac{C \cdot A \cdot R_0}{3.6(0.3T_p + T_{0.3})} \quad (4)$$

where Q_p represents the peak flood discharge, C is the runoff coefficient, A is the watershed area, R_0 is the effective unit rainfall, T_p is the time to peak, and $T_{0.3}$ represents the time required for the recession limb to decrease to 30% of the peak discharge.

From a hydrodynamic perspective, flood propagation and inundation mapping in open channels are governed by the principles of conservation of mass and momentum, mathematically expressed as the one-dimensional (1D) Saint-Venant equations [20]. These equations form the fundamental theoretical basis in the Hydrologic Engineering Center's River Analysis System (HEC-RAS) for simulating unsteady flow conditions [20]. The numerical solution enables the simulation of water level profiles, hydraulic interactions, and backwater effects along the drainage network. The governing equations are formulated as follows:

$$\frac{\partial A}{\partial t} + \frac{\partial Q}{\partial x} = 0 \quad (5)$$

$$\frac{\partial Q}{\partial t} + \frac{\partial (Q^2/A)}{\partial x} + gA\left(\frac{\partial H}{\partial x} + S_f\right) = 0 \quad (6)$$

where the first and second equations represent the continuity and momentum equations, respectively. A represents the flow cross-sectional area, t is time, Q is the flow discharge, x is the longitudinal distance along the channel, g is the gravitational acceleration, H is the water surface elevation, and S_f is the friction slope.

2.4 Calculation and Simulation

The analytical procedure consisted of two sequential phases: hydrological calculation and hydraulic simulation, as summarized in the workflow presented in **Figure 3**. The hydrological analysis began with subwatershed delineation and land-use characterization using GIS-based spatial analysis. Based on these datasets, the composite runoff coefficient was determined, followed by design rainfall estimation through frequency analysis in accordance with SNI 2415:2026. The resulting design rainfall was subsequently transformed into design flood hydrographs using the Nakayasu Synthetic Unit Hydrograph (SUH), which is widely adopted for design flood estimation in Indonesian watersheds [18], [19].

The generated flood hydrographs were then employed as upstream boundary conditions in the HEC-RAS unsteady flow model, while the surveyed channel geometries and drainage network

configuration were incorporated into the hydraulic model [20]. Simulations were conducted for each design return period to evaluate channel conveyance capacity, analyze water surface profiles, identify backwater propagation, and quantify the influence of downstream river stages on the performance of the local drainage system [8], [20], [21]. Finally, the simulated hydraulic characteristics—including water levels, flow velocities, inundation extent, and reverse-flow conditions—were interpreted to identify hydraulic deficiencies and formulate appropriate structural mitigation strategies for improving urban drainage performance and flood resilience [10].

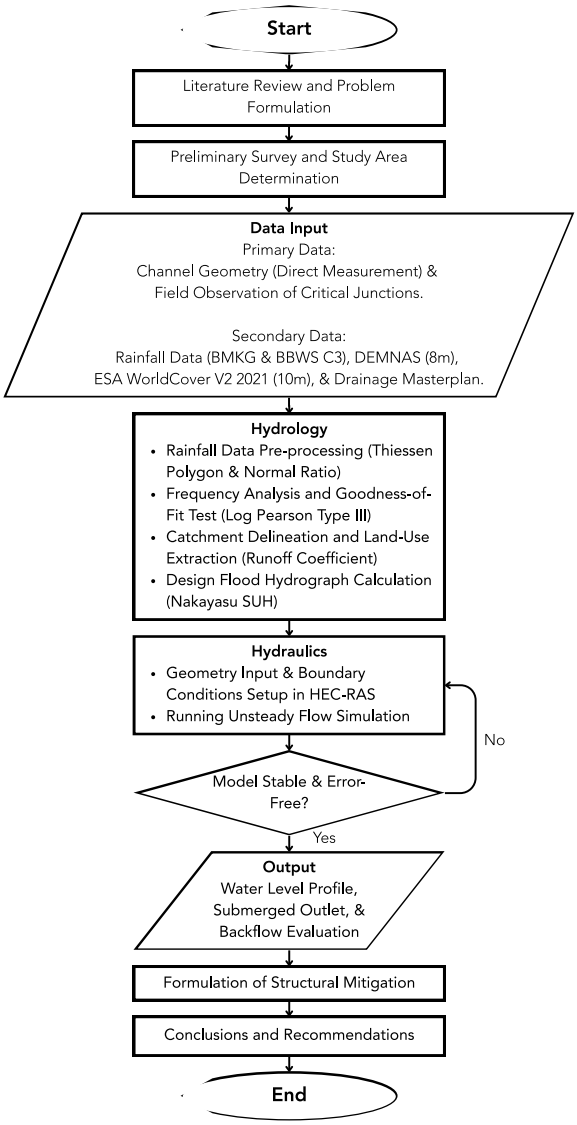
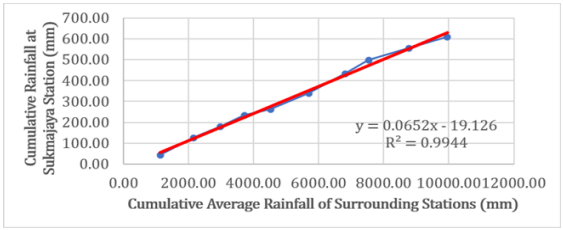


Figure 3. Flowchart of the overall research methodology encompassing hydrological calculations and hydrodynamic simulations

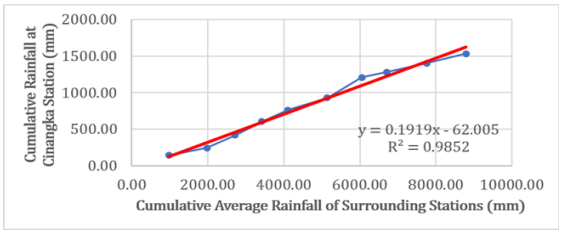
3 Results and Discussion

3.1 Hydrological Analysis and Design Flood

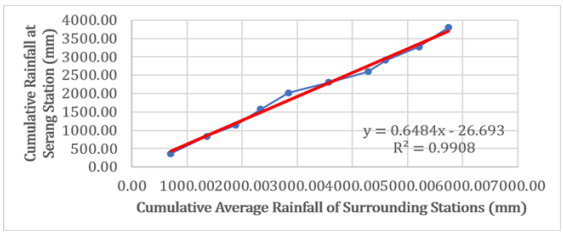
The historical daily rainfall records obtained from the Serang, Puloampel, Sukmajaya, and Cinangka rainfall stations were successfully preprocessed to ensure data completeness and consistency prior to hydrological analysis. Missing observations were estimated using the Normal Ratio method, while data consistency was evaluated using the Double Mass Curve (DMC) analysis. As illustrated in **Figure 4**, the cumulative rainfall relationships exhibit nearly linear trends without noticeable breaks in slope, indicating that the historical rainfall records are sufficiently consistent and reliable for subsequent frequency analysis.



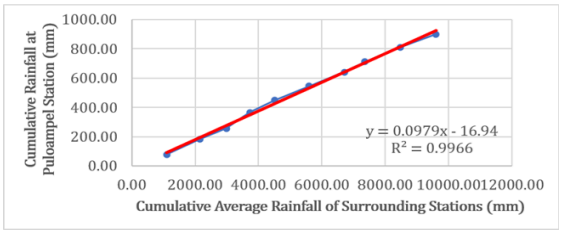
(a) sukmajaya



(b) cinangka



(c) serang



(d) puloampel

Figure 4. Double Mass Curve (DMC) consistency analysis of the rainfall records at the four rainfall stations: (a) Serang; (b) Puloampel; (c) Sukmajaya; and (d) Cinangka

Following the validation of rainfall consistency, the spatial distribution of rainfall over the Cibeber Subwatershed was represented using the Thiessen Polygon method. The calculated influence area of each rainfall station produced different weighting factors

according to its spatial coverage within the watershed, as summarized in **Table 2**. These weighting factors formed the basis for estimating representative areal rainfall used in the subsequent design rainfall analysis.

Table 2. Thiessen polygon influence areas and weighting factors for the rainfall stations

Rain Gauge Station	Influence Area (km^2)	Weighting Factor (%)
Sukmajaya	126.92	88.72
Cinangka	0.61	0.43
Serang	13.69	9.57
Puloampel	1.84	1.29
Total	143.06	100

The statistical characteristics of the areal rainfall data were evaluated to identify the most appropriate probability distribution for estimating design rainfall. The calculated coefficients of skewness (Cs), kurtosis (Ck), and logarithmic skewness (Cs-log) are summarized in **Table 3**. The results indicate that the rainfall dataset did not satisfy the applicability criteria of the Normal and Gumbel distributions. Accordingly, the Log Pearson Type III distribution was selected for subsequent frequency analysis based on the statistical selection criteria specified in SNI 2415:2026. The selection of an appropriate probability distribution is an important step in design flood estimation, as the resulting design rainfall directly influences the magnitude of the subsequent flood hydrograph [19], [22]. In the present study, the positive skewness of the observed rainfall records supports the use of the Log Pearson Type III distribution to represent the probabilistic characteristics of extreme rainfall events within the Cibeber Subwatershed.

Table 3. Statistical parameters of the areal rainfall data

Statistical Parameter	Symbol	Calculated Value
Coefficient of Skewness	C_s	0.319
Coefficient of Kurtosis	C_k	3.452
Logarithmic Skewness	$C_{s\text{-}log}$	-0.293

The suitability of the selected Log Pearson Type III distribution was evaluated using the Chi-Square (χ^2) and Smirnov-Kolmogorov goodness-of-fit tests in accordance with the statistical procedures specified in SNI 2415:2026**.** As summarized in **Table 4**, the calculated test statistics for both methods were lower than their respective critical values at the 5% significance level, indicating that the selected distribution satisfactorily represents the statistical characteristics of the observed rainfall data. Therefore, the Log Pearson Type III distribution was considered statistically acceptable and subsequently adopted for estimating the design rainfall used in the hydrological analysis.

Table 4. Goodness-of-fit test results for the Log Pearson Type III distribution

Test Method	Calculated Value	Critical Value (5%)	Conclusion
Chi Square	0.400	3.841	Accepted
Smirnov-Kolmogorov	0.076	0.410	Accepted

Following the successful goodness-of-fit evaluation, the design rainfall depths were estimated for the 2-, 5, 10-, 25-, and 50-year return periods using the Log Pearson Type III distribution. The calculated design rainfall values are presented in **Table 5**. As expected, the estimated rainfall depth increases progressively with longer return periods, reflecting the lower probability of occurrence associated with increasingly extreme rainfall events. A similar return-period-based approach has been applied in flood design studies in Cilegon, where design flood discharges were estimated for multiple return periods to support subsequent hydraulic assessment [22]. These design rainfall estimates subsequently served as the primary hydrological input for constructing the design flood hydrographs used in the hydraulic analysis, consistent with the general hydrological modelling framework applied in previous flood studies [19].

Table 5. Design rainfall for various return periods

Return Periode (Years)	Design Rainfall (mm)
2	90.95
5	105.47
10	113.96
25	123.77
50	130.55

Following the estimation of the design rainfall, the land-use characteristics of the Cibeber Subwatershed were analyzed to quantify the watershed response through the determination of a composite runoff coefficient. The land-use analysis reveals that the watershed is predominantly covered by tree cover, followed by agricultural and built-up areas, indicating a heterogeneous catchment with varying hydrological responses. Previous studies have similarly demonstrated that differences in land-use and land-cover characteristics can influence surface runoff generation, with changes in forest, agricultural, and built-up areas affecting the hydrological response of a watershed [2], [3]. Since each land-cover type exhibits different infiltration and runoff characteristics, an appropriate runoff coefficient was assigned to each category in accordance with SNI 2415:2026. The land-use composition, corresponding

areas, and assigned runoff coefficients are summarized in **Table 6**.

Table 6. Land-use composition and assigned runoff coefficients of the cibeber subwatershed

Land Use Type	Area (Ha)	Percentage (%)	Runoff Coefficient (C)
Tree Cover	1903.39	47.43%	0.30
Grassland	414.35	10.32%	0.35
Cropland	322.87	8.05%	0.40
Built-up	1326.63	33.06%	0.95
Bare/Sparse Vegetation	33.9	0.84%	0.70
Permanent Water Bodies	9.54	0.24%	1.00
Herbaceous Wetland	2.51	0.06%	0.85
	4013.19	100%	0.533

To develop the design rainfall hyetograph required for the Nakayasu Synthetic Unit Hydrograph (SUH), the calculated daily design rainfall was temporally distributed into hourly rainfall depths using the Mononobe method. Based on the estimated watershed time of concentration of 6 hours, the rainfall depths were proportionally allocated into six consecutive hourly intervals. Subsequently, the hourly rainfall depths were multiplied by the composite runoff coefficient (C = 0.533) obtained from the land-use analysis to derive the effective rainfall used as the hydrological input for the flood hydrograph simulation. This procedure follows the general framework of converting design rainfall into effective rainfall as the input for synthetic unit hydrograph-based flood estimation [19]. The resulting effective hourly rainfall distributions for each design return period are summarized in **Table 7**.

Table 7. Effective hourly rainfall distributions derived from the Mononobe temporal rainfall distribution

Hour (t)	Distribution Ratio (%)	2-Year (mm/hr)	5-Year (mm/hr)	10-Year (mm/hr)	25-Year (mm/hr)	50-Year (mm/hr)
1	55.03	26.68	30.94	33.43	36.30	38.29
2	14.30	6.93	8.04	8.69	9.44	9.95
3	10.03	4.86	5.64	6.09	6.62	6.98
4	7.99	3.87	4.49	4.85	5.27	5.56
5	6.75	3.27	3.79	4.10	4.45	4.69
6	5.90	2.86	3.31	3.58	3.89	4.10
Total	100	48.48	56.21	60.74	65.97	69.58

Figure 5 presents the simulated Nakayasu Synthetic Unit Hydrographs (SUH) for the selected return periods. As expected, increasing return periods produced progressively higher peak discharges and longer recession limbs, indicating a stronger hydrological response of the Cibeber Subwatershed under more extreme rainfall conditions. The simulated peak discharge increased from 62.82 m^3/s for the 2-year event to 84.92 m^3/s for the 50-year event, representing approximately a 35% increase in peak flow. This increasing peak-discharge response is consistent with the application of the Nakayasu SUH in previous flood studies, where the method was used to estimate design flood hydrographs across different return periods and produced peak discharge estimates comparable with other hydrological and numerical approaches [19]. The corresponding peak discharge values for each return period are summarized in **Table 8**. These design hydrographs subsequently served as the upstream boundary conditions in the unsteady-flow HEC-RAS simulations to evaluate the hydraulic performance of the existing drainage system under various flood scenarios.

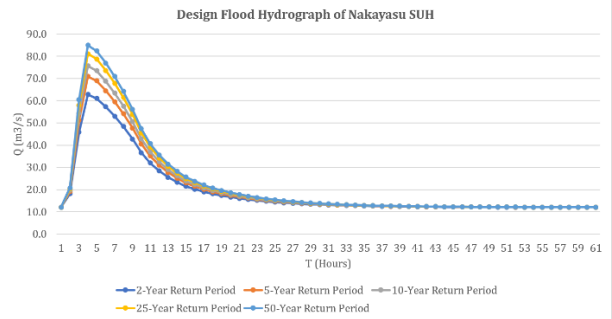


Figure 5. Design flood hydrographs using the Nakayasu SUH method for various return periods

Table 8. Simulated peak discharges for the selected design return periods

Return Period (years)	Design Rainfall (mm)	Peak Discharge (m^3/s)
2	90.95	62.82
5	105.47	70.92
10	113.96	75.66
25	123.77	81.13
50	130.55	84.92

3.2 Geometric Inventory and Existing Drainage Conditions

An accurate representation of the existing drainage network is fundamental for developing a reliable hydraulic model. Therefore, an inventory of the primary drainage system was first established using the official drainage inventory obtained from the Department of Public Works and Spatial Planning (DPUPR) of Cilegon City. This database was used to identify the channel network, connectivity, and upstream–downstream flow directions within the study area. The inventory was subsequently verified through field surveys to measure the actual channel dimensions and document field conditions, while channel lengths were confirmed using high-resolution satellite imagery in Google Earth. This verification process ensured that the hydraulic model accurately represented the existing drainage configuration rather than relying solely on administrative records. The compiled geometric characteristics of the evaluated drainage channels are summarized in **Table 9** and served as the geometric basis for the subsequent HEC-RAS simulations.

Table 9. Inventory of the evaluated drainage network

Channel Name	Section Start/End	Channel Length (m)	Width (m)
Cibeber River	Cikerai – Muara Terate	14,900	9
Kubang Laban Secondary Channel	Sawah Besar – Semendaran	2,660	3
Kubang Mayit Secondary Channel	Ketileng Wetan – Nyikambang	2,000	4
Seneja Secondary Channel	Temu Putih – Nyikambang	3,000	3
Kranggot Tertiary Channel	Seneja Secondary Channel – Kubang Laban Secondary Channel	1,100	1.5

Representative channel cross-sections were selected to illustrate the geometric characteristics adopted in the hydraulic model. **Figure 6** presents the surveyed cross-section of the Cibeber River (RS 275), which was used as a representative geometric input for HEC-RAS. The surveyed dimensions define the channel geometry required for hydraulic computations, including flow area, wetted perimeter, and water-surface elevation during the simulation. The corresponding field photograph is presented in **Figure 7** to verify the surveyed dimensions and document the existing physical condition of the channel. Although only one representative location is presented for illustration, the same survey methodology and geometric verification procedure were consistently applied to all drainage channels incorporated into the hydraulic model, ensuring a consistent representation of the existing drainage system.

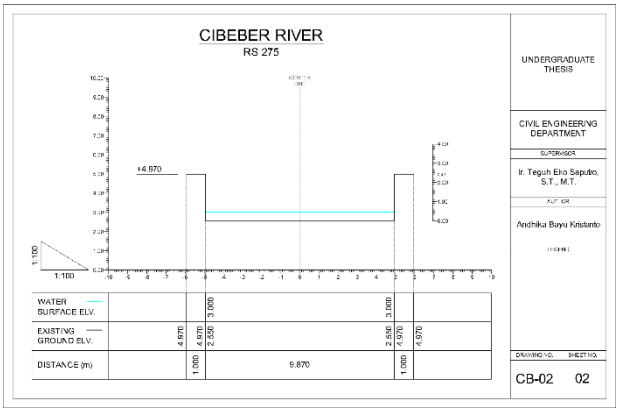


Figure 6. Representative field-surveyed cross-section of the cibeber river (RS 275) used as geometric input for the HEC-RAS hydraulic model



Figure 7. Field photograph of the representative survey location at the cibeber river (RS 275), showing the existing channel condition

3.3 Hydraulic Simulation and Backwater Interaction

Hydraulic performance of the existing drainage network was evaluated using unsteady-flow simulations in HEC-RAS under the 2, 5, 10, 25, and 50-year design flood scenarios. The simulations were performed to examine the progressive hydraulic response of the drainage system as the design discharge increased, with particular emphasis on the downstream junction between the Kubang Laban secondary channel (RS 0) and the Cibeber River (RS 0), where the interaction between the local drainage system and the receiving river governs flow conditions. Such river–drainage interactions have been identified in previous studies as an important factor influencing urban drainage performance, particularly when elevated receiving-river stages

constrain drainage outflow and increase the potential for backwater and flow reversal [6], [8]. The principal hydraulic responses at this critical junction are summarized in **Table 10**, including the simulated junction water surface elevation and the flow velocities in both the secondary channel and the receiving river. Among the evaluated return periods, the Q50 event produced the most critical hydraulic condition and is therefore presented in greater detail in the subsequent figures.

Table 10. Hydraulic characteristics at the kubang laban–cibeber junction under different design flood scenarios

Return Period	Peak Flow in Cibeber (m^3/s)	Water Surface Elevation at Junction (m)	Kubang Laban Velocity (m/s)	Cibeber Velocity (m/s)
Q2	61.74	4.85	0.04	1.82
Q5	69.67	5.07	0.04	1.87
Q10	74.71	5.21	0.04	1.90
Q25	79.66	5.35	0.04	1.92
Q50	83.36	5.46	0.03	1.94

As summarized in **Table 10**, the simulated hydraulic response consistently demonstrates that increasing design discharges resulted in progressively higher water-surface elevations at the downstream junction. The maximum water level increased from 4.85 m during the Q2 event to 5.46 m under the Q50 scenario, closely following the rise of the Cibeber River stage. Identical water-surface elevations were obtained at both the Kubang Laban outlet and the adjacent Cibeber River section throughout all simulated return periods, indicating that hydraulic conditions at the outlet were governed primarily by the downstream river stage rather than by the discharge capacity of the local drainage channel. This finding is consistent with previous studies showing that elevated receiving-river water levels can substantially reduce the drainage capacity of urban outfalls and, under sufficiently high downstream stages, induce backflow into the drainage network [6]. A similar river–drainage interaction was also reported in previous research, where the water level of the receiving river influenced the performance of a connected drainage channel and contributed to overtopping and backwater effects [8]. Consequently, the simulated water levels exceeded the existing channel-bank elevation (approximately 3.60 m) even under the Q2 event, while the magnitude of overtopping became progressively more severe with increasing return period. The representative cross-sectional water-surface profile during the Q50 simulation is presented in **Figure 8**.

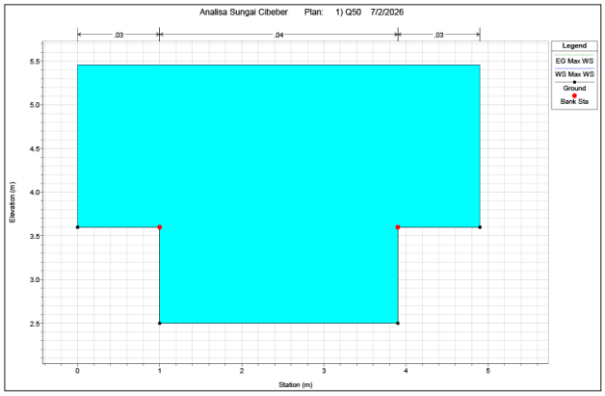


Figure 8. Simulated cross-sectional water-surface profile at the kubang laban outlet (RS 0) during the Q50 event, showing channel overtopping induced by elevated water levels in the cibeber river

Although the cross-sectional profile confirms the occurrence of overtopping, it does not fully explain the hydraulic mechanism responsible for the observed flooding. During the Q50 simulation, the elevated stage of the Cibeber River submerged the outlet of the Kubang Laban secondary channel, preventing gravity-driven outflow and producing a prolonged backwater condition. This hydraulic interaction is illustrated by the three-dimensional (3D) perspective view presented in **Figure 9**, which clearly demonstrates the upstream propagation of elevated water levels from the receiving river into the local drainage network. These findings confirm that the flooding mechanism was governed primarily by downstream hydraulic control rather than by the conveyance capacity of the secondary channel alone.

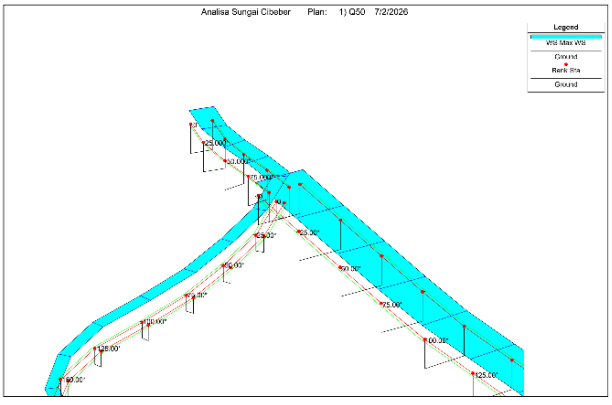


Figure 9. Three-dimensional (3D) perspective of the kubang laban–cibeber junction during the Q50 simulation, illustrating the submerged outlet and upstream propagation of backwater into the secondary drainage channel

The temporal variation in discharge and flow velocity at the Kubang Laban outlet further confirms the influence of downstream backwater on the drainage performance. A summary of the simulated hydraulic conditions during the Q50 event is presented in **Table 11**. As the water level in the

Cibeber River increased, the discharge capacity of the secondary channel progressively decreased until gravity-driven outflow was completely suppressed. During the peak flood stage, the simulated discharge reached -2.02 m^3/s, accompanied by a flow velocity of -0.28 m/s. Rather than indicating a reduction in discharge magnitude alone, the negative values signify a complete reversal of the flow direction, demonstrating that floodwater from the Cibeber River propagated upstream into the Kubang Laban drainage channel. A comparable hydraulic response has been reported in previous studies, where elevated receiving-river water levels progressively reduced drainage capacity and eventually induced backflow into connected urban drainage systems [6]. Similarly, river–drainage interactions have been shown to generate backwater and overtopping when elevated river stages constrain drainage outflow [8]. In the present study, the occurrence of negative discharge provides direct evidence that the downstream river stage not only restricted gravity-driven drainage but temporarily reversed the flow direction, demonstrating a pronounced backwater effect controlling the flooding process within the Sukmajaya drainage system.

Table 11. Temporal hydraulic response at the Kubang Laban outlet (RS 0) during the Q50 simulation

Time (hh:mm)	Discharge (m³/s)	Velocity (m/s)	Hydraulic Condition
01:00	0.09	0.03	Restricted Outflow
02:00	-2.02	-0.28	Reverse Flow
10:00	0.79	0.13	Flow Recovery
18:00	0.45	0.14	Normal Outflow

The temporal variation in water surface elevation further explains the hydraulic mechanism responsible for the observed backwater effect. As illustrated in **Figure 10**, the water level in the Cibeber River rose rapidly during the rising limb of the flood hydrograph and remained consistently higher than that at the Kubang Laban outlet throughout the critical period. This persistent downstream stage dominance prevented gravity-driven discharge from the secondary channel, resulting in prolonged outlet submergence and reverse-flow conditions observed during the simulation. Similar river–drainage interactions have been reported in previous studies, where elevated receiving-river stages reduced drainage outflow capacity and maintained backwater conditions at urban drainage outlets [6], [8]. These findings indicate that the temporal dominance of the receiving-river stage can be a critical control on drainage performance when local outfalls are hydraulically connected to the river system. The comparison confirms that flooding within the Sukmajaya drainage system was governed primarily by downstream hydraulic control rather than by insufficient local channel capacity alone.

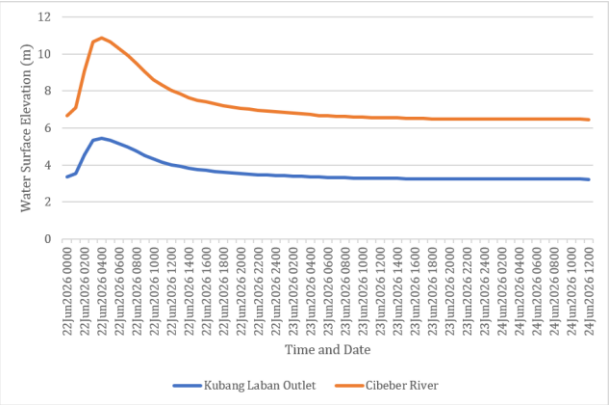


Figure 10. Comparison of simulated water surface elevations at the Kubang Laban outlet and the Cibeber River during the Q50 event, illustrating the prolonged downstream stage dominance responsible for the backwater effect

Overall, the hydraulic simulations consistently indicate that the flooding observed in the Sukmajaya drainage system is governed by downstream hydraulic control exerted by the Cibeber River rather than by the conveyance capacity of the local drainage channels alone. Increasing river stages progressively submerged the Kubang Laban outlet, leading to overtopping, reduced conveyance efficiency, flow stagnation, and temporary reverse flow during the peak flood period. These hydraulic responses collectively indicate that the predominant flooding mechanism is a backwater effect induced by the receiving river. This finding is consistent with previous studies demonstrating that elevated receiving-river stages can constrain urban drainage outflows and induce backflow when drainage outlets become hydraulically submerged [6], [8]. Consequently, improving flood resilience in the study area requires mitigation measures that address downstream hydraulic conditions—such as preventing reverse flow or regulating river stages—in addition to conventional drainage capacity improvements.

3.4 Mitigation Strategies and Flood Control Interventions

The hydraulic simulations demonstrated that overtopping occurred under all evaluated design flood scenarios, with the maximum water surface elevation at the Kubang Laban outlet increasing from 4.85 m during the Q2 event to 5.46 m during the Q50 event. During the most critical condition, the outlet remained submerged for approximately 16 hours, while the discharge at the junction reversed to -2.02 m^3/s, indicating that floodwater propagated from the Cibeber River into the local drainage network. These findings indicate that flooding within the Sukmajaya

drainage system is primarily governed by downstream backwater effects rather than by insufficient channel capacity alone. Therefore, the proposed mitigation strategy focuses on interrupting the hydraulic interaction between the Cibeber River and the local drainage system through an integrated structural approach. This approach is consistent with integrated urban flood management strategies that combine hydraulic protection, temporary storage, and controlled drainage to reduce flood exposure and maintain drainage functionality under elevated downstream water levels [23], [24].

The first proposed measure is the construction of continuous levees along the lower reach of the Cibeber River and the downstream section of the Kubang Laban channel. Considering that overtopping occurred even under the Q2 event, the primary function of the levees is to hydraulically isolate the local drainage system from elevated river stages rather than merely increasing channel capacity. By preventing lateral overtopping and limiting the direct hydraulic influence of the Cibeber River at the drainage outlet, the levees would help reduce the propagation of elevated river stages into the surrounding drainage network. Similar structural flood-protection approaches have been incorporated into urban polder systems to reduce the exposure of low-lying drainage areas to elevated external water levels [23].

Nevertheless, isolating the drainage system also eliminates gravity-driven discharge whenever the downstream river stage exceeds the outlet elevation. Because the hydraulic simulations indicated that the outlet remained submerged for approximately 16 hours during the Q50 event, temporary storage is required to accommodate runoff generated within the catchment while discharge to the receiving river is restricted. Therefore, a retention storage facility functioning as a polder reservoir is proposed to temporarily retain runoff until downstream water levels recede, thereby maintaining storage capacity during periods of restricted outflow. The use of temporary detention or in-line storage to accommodate stormwater while downstream hydraulic conditions are unfavorable has also been investigated in previous urban drainage studies [24].

Finally, a pumping station becomes an essential component of the proposed mitigation system because gravity drainage cannot operate while the outlet remains submerged. The simulated reverse discharge reaching -2.02 m^3/s demonstrates that flow direction at the outlet was completely reversed during the flood peak, making passive drainage ineffective during the critical period. Consequently, mechanical pumping is proposed to transfer the stored runoff from the retention facility across the levee into the Cibeber River until downstream water levels recede and gravity-driven drainage can resume. Previous studies of urban drainage systems have similarly considered pumping and hydraulic control measures as means of maintaining drainage performance under extreme rainfall and constrained downstream conditions [25]. Accordingly, the proposed mitigation framework integrates levee protection, temporary retention storage, and mechanical pumping to interrupt the adverse river–drainage interaction identified in the hydraulic simulations.

It should be noted that the proposed mitigation strategy remains conceptual because no post-mitigation hydraulic simulations were performed in the present study. Therefore, future studies are recommended to evaluate the hydraulic performance of the proposed levee, retention storage, and pumping system through scenario-based HEC-RAS simulations to optimize their dimensions and operational configurations before implementation.

4 Conclusion

This study evaluated the hydraulic performance of the Sukmajaya urban drainage system under multiple design flood scenarios using integrated hydrological and unsteady-flow hydraulic modeling. The results demonstrate that flooding within the study area is governed primarily by hydraulic interaction between the local drainage network and the Cibeber River rather than by insufficient channel capacity alone. Under the Q50 design flood, corresponding to a peak inflow of 84.92 m^3/s, the downstream river stage increased the maximum water surface elevation at the Kubang Laban outlet to 5.46 m, maintained a submerged outlet condition for approximately 16 hours, and generated reverse flow reaching -2.02 m^3/s. These findings provide clear evidence that downstream backwater is the dominant mechanism controlling flood occurrence in the Sukmajaya drainage system.

Consequently, conventional channel enlargement alone would not effectively mitigate flooding because the primary hydraulic constraint originates from the downstream boundary condition imposed by the receiving river. Instead, flood mitigation should focus on interrupting hydraulic connectivity between the drainage network and the Cibeber River while preserving the functionality of the local drainage system during elevated river stages. Accordingly, this study recommends an integrated polder system consisting of continuous levees, temporary retention storage, and mechanical pumping as a conceptual flood mitigation strategy for the study area. Although the proposed mitigation strategy has not yet been evaluated through post-improvement hydraulic simulations, the presented framework provides a technically justified basis for future optimization and may serve as a practical reference for flood management in other urban areas experiencing similar river-induced backwater conditions.

5 Acknowledgement

The authors would like to express their deepest gratitude to the Department of Civil Engineering, Universitas Serang Raya, for the academic support and guidance provided during the course of this study. Special appreciation is extended to the Department of Public Works and Spatial Planning (DPUPR) of Cilegon City, specifically the Water Resources Division, for granting the research permission and providing essential geometric inventories, spatial KML data of the drainage networks, and the established channel hierarchies. The authors also sincerely thank the Serang Class I Maritime Meteorology Station (BMKG) and the Cidanau-Ciujung-Cidurian River Basin Territory Organization (BBWS C3) for the provision of crucial rainfall data. Furthermore, the authors thank the academic advisors and examiners for their invaluable technical feedback and constructive critiques, which significantly improved the quality of this manuscript.

References

[1] T. A. Shaikh, G. E. Adjovu, H. Stephen, and S. Ahmad, "Impacts of urbanization on watershed hydrology and runoff water quality of a watershed: a review," in *World Environmental and Water Resources Congress 2023*, 2023, pp. 1271–1283.

[2] I. S. Astuti, K. Sahoo, A. Milewski, and D. R. Mishra, "Impact of land use land cover (LULC) change on surface runoff in an increasingly urbanized tropical watershed," *Water Resources Management*, vol. 33, no. 12, pp. 4087–4103, 2019.

[3] P. C. Pertiwi, E. S. Hisyam, and D. Yofianti, "The effect of land use change to surface runoff discharge in the POMPONG watershed at Bangka regency," in *IOP Conference Series: Earth and Environmental Science*, IOP Publishing, 2020, p. 12039.

[4] G. A. Hodgkins, R. W. Dudley, S. A. Archfield, and B. Renard, "Effects of climate, regulation, and urbanization on historical flood trends in the United States," *J. Hydrol. (Amst).*, vol. 573, pp. 697–709, 2019.

[5] T.-H. Nguyen, "Linking climate change to urban storm drainage system design: An innovative approach to modeling of extreme rainfall processes over different spatial and temporal scales," *Journal of Hydro-environment Research*, vol. 29, pp. 80–95, 2020.

[6] H. Zhang, J. Liu, C. Mei, J. Wang, and T. Song, "Quantifying the impact of river levels on urban drainage capacity," *Water Resources Management*, vol. 39, no. 14, pp. 7593–7621, 2025.

[7] A. K. B. De Oliveira *et al.*, "Evaluating the role of urban drainage flaws in triggering cascading effects on critical infrastructure, affecting urban resilience," *Infrastructures (Basel).*, vol. 7, no. 11, p. 153, 2022.

[8] F. Yustiana, M. H. Ridwanullah, Y. N. Kurniadi, E. Wardhani, and E. Widyaningsih, "HEC-RAS model for drainage capacity analysis and peak discharge simulation of Cimande River," *Geomate Journal*, vol. 27, no. 123, pp. 30–37, 2024.

[9] A. S. Abdurrasheed, K. W. Yusof, H. B. Takaijudin, A. Ab, and B. S. Iskandar, "Effects of backwater on hydraulic performance evaluation of rainsmart modules in sustainable drainage systems," in *Proceedings of the 4th International Conference on Water Resources, Langkawi, Malaysia*, 2018, pp. 17–21.

[10] C. R. Ferguson and R. A. Fenner, "The potential for natural flood management to maintain free discharge at urban drainage outfalls," *J. Flood Risk Manag.*, vol. 13, no. 3, p. e12617, 2020.

[11] S. Afrin, M. M. Islam, and M. M. Rahman, "Adequacy assessment of an urban drainage system considering future land use and climate change scenario," *Journal of Water and Climate Change*, vol. 12, no. 5, pp. 1944–1957, 2021.

[12] PortalNusantara.id, "Banjir Rendam Permukiman Warga di Kranggot Cilegon, 241 KK Terdampak." Accessed: Jul. 03, 2026. [Online]. Available: https://www.portalnusantara.id/banjir-rendam-permukiman-warga-di-kranggot-cilegon-241-kk-terdampak

[13] Pemerintah Kota Cilegon, "Susuri Banjir di Kranggot, Wali Kota Robinsar Instruksikan Pengoptimalan Bantaran Sungai :: Berita Cilegon." Accessed: Jul. 03, 2026. [Online]. Available: https://berita.cilegon.go.id/baca/Susuri-Banjir-di-Kranggot,-Wali-KotaRobinsar-Instruksikan-Pengoptimalan-Bantaran-Sungai/20260414/MTcyNTU1

[14] A. Sopian, "Banjir dari Kali Pasar Kranggot Cilegon Bawa Sampah ke Pemukiman Warga · Faktabanten.co.id." Accessed: Jul. 03, 2026. [Online]. Available: https://faktabanten.co.id/cilegon/banjir-dari-kali-pasar-kranggot-cilegon-bawa-sampah-ke-pemukiman-warga/

[15] V. Te Chow, *Open-Channel Hydraulics*. New York: McGraw-Hill, 1959.

[16] B. W. Mutaqin, M. N. Isnain, M. A. Marfai, H. Fatchurohman, A. Quesada-Román, and N. Khakhim, "Assessing the accuracy of open-source digital elevation models for the geomorphological analysis of very small islands of Indonesia," *Applied Geomatics*, vol. 15, no. 4, pp. 957–974, 2023.

[17] P. Xu *et al.*, "Comparative validation of recent 10 m-resolution global land cover maps," *Remote Sens. Environ.*, vol. 311, p. 114316, 2024.

[18] Badan Standardisasi Nasional (BSN), "SNI 2415:2026, Tata Cara Perhitungan Debit Banjir Rencana," Jakarta, 2026.

[19] M. B. Ansori, U. Lasminto, and A. A. G. Kartika, "Flood hydrograph analysis using synthetic unit hydrograph, HEC-HMS, and HEC-RAS 2D unsteady flow precipitation on-grid model for disaster risk mitigation," *Geomate Journal*, vol. 25, no. 107, pp. 50–58, 2023.

[20] Hydrologic Engineering Center, "HEC-RAS, River Analysis System: User's Manual," Davis, CA, 2021.

[21] R. R. Syafri, M. P. Hadi, and S. Suprayogi, "Hydrodynamic modelling of Juwana River flooding using HEC-RAS 2D," in *IOP Conference Series: Earth and Environmental Science*, IOP Publishing, 2020, p. 12028.

[22] S. R. F. S. Waita, B. A. Priyambodho, N. P. Purnaditya, W. Fathonah, S. Subekti, and F. Nabila, "Flood Analysis of the Kedung Ingas River and Pabean River the Cilegon City," *Fondasi : Jurnal Teknik Sipil*, vol. 14, no. 1, pp. 47–58, 2025, [Online]. Available: https://jurnal.untirta.ac.id/index.php/jft/article/view/32284

[23] Y. Budiyono, M. A. Marfai, J. Aerts, H. de Moel, and P. J. Ward, "Flood risk in polder Systems in Jakarta: Present and future analyses," in *Disaster Risk Reduction in Indonesia: Progress, Challenges, and Issues*, Springer, 2017, pp. 517–537.

[24] N. Kändler, I. Annus, A. Vassiljev, and R. Puust, "Real time controlled sustainable urban drainage systems in dense urban areas," *Journal of Water Supply: Research and Technology—AQUA*, vol. 69, no. 3, pp. 238–247, 2020.

[25] T. Ma, J.-S. Kim, C. Jun, Y.-I. Moon, and H. Moon, "Optimizing urban flood management: enhancing urban drainage system efficiency under extreme rainfall events," *Journal of Hydroinformatics*, vol. 26, no. 11, pp. 2704–2719, 2024.